NANO LETTERS

2007
Vol. 7, No. 5
1165−1171

Simultaneous Self-Assembly, Orientation, and Patterning of Peptide–Amphiphile Nanofibers by Soft Lithography

Albert M. Hung[†] and Samuel I. Stupp*[,†,‡,§]

Department of Materials Science and Engineering, Department of Chemistry, and Feinberg School of Medicine, Northwestern University, 2220 Campus Drive, Evanston, Illinois 60208-3108

Received December 5, 2006; Revised Manuscript Received April 9, 2007

ABSTRACT

Self-assembled nanofibers of peptide–amphiphile molecules have been of great interest because of their bioactivity both in vitro and in vivo. In this work, we demonstrate the simultaneous self-assembly, alignment, and patterning of these nanofibers over large areas by a novel technique termed sonication-assisted solution embossing. In this soft lithographic technique, the nanostructures self-assemble by solvent evaporation while under the influence of ultrasonic agitation and confinement within the topographical features of an elastomeric stamp. The nanofibers orient parallel to the channels as they assemble out of solution, yielding bundles of aligned nanofibers on the substrate after the stamp is removed. Alignment is likely a result of steric confinement and possibly a transition to a lyotropic liquid crystalline phase as solvent evaporates. This technique is not limited to uniaxial alignment and is shown to be able to guide nanofibers around turns. Alignment of nanostructures by this method introduces the possibility of controlling macroscale cellular behavior or material properties by tuning the directionality of interactions at the nanoscale.

Controlling the placement and orientation of nanometer-scale objects is essential for many of the technological applications envisioned for supramolecular self-assembly.[1−3] Most self-assembling materials are macroscopically disordered which can limit their bulk properties and potential uses. Patterning on the microscale may extend order in a predictable manner over large areas, dramatically improving performance and enabling new functions.[4−9] Many strategies have been investigated for controlling order in materials, and some of these, including graphoepitaxy[10] and soft lithographic micromolding,[11−14] rely on the effects that spatial confinement have on the behavior of materials. These techniques take advantage of the strengths of top−down fabrication such as materials generality and facile control of feature shape and pattern and apply them to a bottom−up system. The idea of using spatial confinement to guide micro- or nanoscale ordering has been extensively applied to self-organized systems, including block copolymers,[8−10,15,16] colloidal crystals,[17,18] and liquid crystals.[19−22] However, systems that assemble into discrete, nanoscale objects from dilute molecular solution present a unique challenge because they often have poor mobility in the neat phase and therefore must be patterned while solvated. Some of these materials have been aligned by electric fields,[14,23,24] Langmuir−Blodgett techniques,[25,26] or mixing with liquid crystals,[20,27−29] but these methods are limited in the patterns and molecular orientations they can produce. To our knowledge, the possibility of patterning such systems by spatial confinement as the molecules self-assemble from solution into supramolecular structures has not been reported.

Our interest in patterning is in its application to self-assembling systems for the development of novel materials that are useful, tunable, and easily processed. A class of molecules known as peptide−amphiphiles (PAs) that consist of an aliphatic tail linked to an oligopeptide segment have been investigated in recent years and shown to assemble into a wide range of one- and two-dimensional supramolecular structures.[30−32] In our laboratory, PAs have been designed that self-assemble into cylindrical nanofibers from aqueous solution by burying their alkyl segments in the core of a nanofiber and displaying their peptide sequences on the surface.[33] Previous studies suggest that β-sheet formation is

* Corresponding author. E-mail: s-stupp@northwestern.edu.
† Department of Materials Science and Engineering.
‡ Department of Chemistry.
§ Feinberg School of Medicine.

10.1021/nl062835z CCC: $37.00
Published on Web 04/21/2007

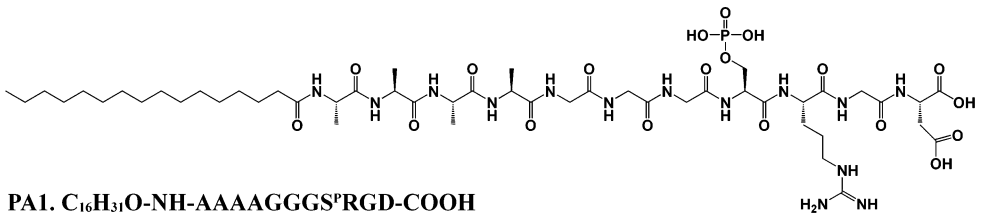

PA1. $C_{16}H_{31}O$-NH-AAAAGGGS^{p}RGD-COOH

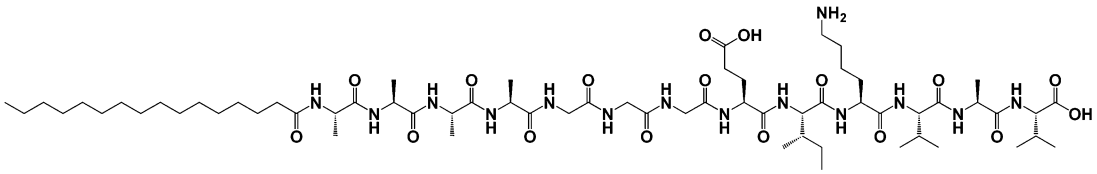

PA2. $C_{16}H_{31}O$-NH-AAAAGGGEIKVAV-COOH

Figure 1. Chemical structures of PA molecules **1** and **2**.

a strong determinant of the cylindrical architecture of the supramolecular assemblies.[34−39] The nanofibers intertwine into three-dimensional networks that have been studied in our laboratory for a variety of applications in regenerative medicine, including biomimetic hydroxyapatite mineralization,[33] neural progenitor cell differentiation,[40] and blood vessel formation.[41]

Work on patterning surfaces with proteins and epitopes is extensive,[42−48] but the one-dimensional structure of the PA nanofibers adds another level of order that may be exploited to control cell behavior or templated mineralization. Alignment of the PA nanofibers would also enable more detailed investigations of their internal structure. The nanofibers assemble readily upon solvent evaporation but are difficult to manipulate when completely dry. Collagen fibrils have been aligned in arrays created by electron-beam lithography[49] and dip-pen nanolithography (DPN).[50] Similarly, we have shown that DPN can produce a low degree of orientation of PA nanofibers but only in small areas.[51]

Soft lithography techniques have proven to be inexpensive and versatile methods for low-temperature patterning of soft matter.[11−14,44,48] Micromolding and liquid embossing using grooves cast from diffraction grating masters allow for facile patterning and confinement of material in dense arrays of submicrometer lines.[52−54] In the present work, we achieve long-range order of PA nanofibers starting from solution prior to their self-assembly and using only spatial confinement. We demonstrate the simultaneous self-assembly, alignment, and patterning of PA nanofibers over an area approaching 1 cm^2 by a sonication-assisted solution embossing technique. The technique is shown not to be limited to unaxial alignment but can be used to guide the nanofibers around corners.

The chemical structures of PA molecules **1** and **2** employed in this study are shown in Figure 1. PA **1** is terminated with the tripeptide RGD, a well-known epitope that among other things can promote cell adhesion.[55,56] PA **2** displays the pentapeptide IKVAV found in laminin-1 that has been demonstrated to promote process outgrowth in neurons.[57,58] Solid-phase synthesis and in vitro studies of PA **1** and **2** have been previously reported.[33−36,40] PA **2** is of interest for its ability to promote and guide neurite outgrowth in the regeneration of the nervous system or in the creation of in vitro assays for neuroscience.

Optical diffraction gratings (Edmund Industrial Optics) with groove densities of 2400 and 3600 lines/mm (line periods of 416 and 278 nm, respectively) were used as master molds to cast patterned poly(dimethylsiloxane) (PDMS) stamps following procedures reported by Roman et al.[53] To improve the fidelity and mechanical stability of the PDMS replica, a composite structure was employed in which the surface features were cast in stiffer PDMS (h-PDMS) and supported with a thick backing of soft PDMS (see Supporting Information).[59] Prior to use, the stamps were cleaned of dust and debris by ultrasonication in 2-propanol and then in deionized water. The stamp was placed on a piece of glass that served as a rigid backing, and a circular weight used to apply a load on the stamp of roughly 30 g/cm^2.

Borosilicate glass or silicon substrates (0.5 mm thick, single side polished, 1500 Ω cm, University Wafer) were cleaned in a hot piranha mixture to render them hydrophilic. A substrate was placed in the bottom of an empty glass beaker immersed in an ultrasonic bath. Four microliters of 1−5% by weight PA solution in water was pipetted onto it, and the weighted PDMS stamp brought down on top of the solution. The circular weight was sized to fit snugly within the glass beaker and prevent excessive translational movement of the stamp. The entire setup was sonicated for 1 h at 40 kHz in a Branson 1510 ultrasonic cleaner and allowed to dry for a day without any further agitation before the stamp was removed. Samples were imaged by tapping mode atomic force microscopy (AFM) using a JEOL 5200 scanning probe microscope. Samples made on glass substrates were examined by AFM and used for cell studies. Scanning electron microscopy (SEM) images were collected on a Hitachi S4500 scanning electron microscope.

Figure 2 shows AFM images of nanofibers of PA **1** embossed from a 5 wt % solution in capillaries with periods of 416 and 278 nm. Qualitatively, the supramolecular

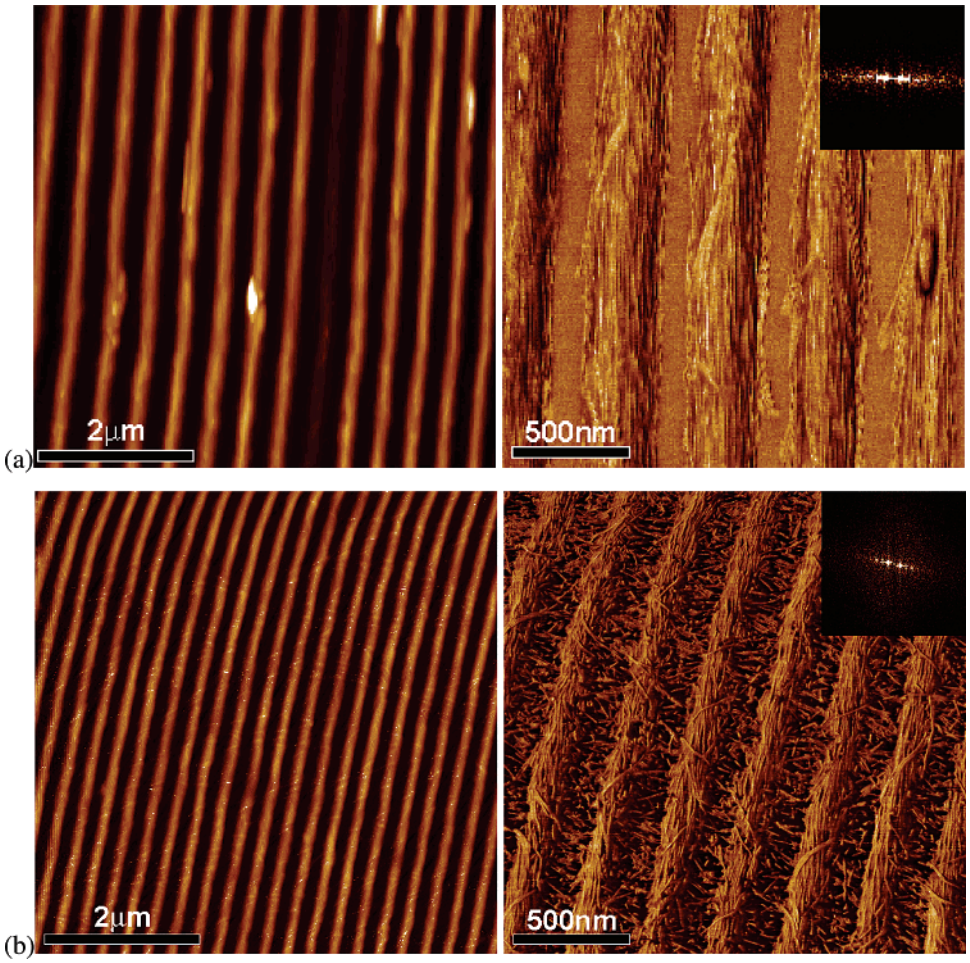

Figure 2. AFM height and phase images of aligned supramolecular nanofibers of PA **1**. The fibers were embossed from a 5 wt % solution into lines with periods of (a) 417 nm and (b) 278 nm (height scales 106 and 99.8 nm, respectively). In (a), the widths of the nanofiber bundles were ca. 200−300 nm, and the average height of the lines was 55.1 ± 0.7 nm. The inset shows a fast Fourier transform (FFT) of the phase image, revealing the periodicity of the grating pattern (brightest spots toward the center) and the nanofibers within each line (diffuse bands to the outside). In (b), the widths were ca. 150 nm, and the average height of the lines was 33.3 ± 1.0 nm. The FFT of the phase image shows similar alignment along the channels as well as some off-axis orientation of the underlying residual layer of nanofibers.

nanofibers conformed to the pattern of the grating and appeared to be very well aligned in long bundles along the direction of the grooves. For the 416 nm lines, most of the bundles were, as in Figure 2a, cleanly separated from each other with no residual layer of nanofibers coating the substrate in between. For the 278 nm lines, there was a ubiquitous residual layer of nanofibers between the nanofiber bundles, but excellent alignment within the bundles was still observed and the uniformity of deposition was very good.

AFM images of PA **2** nanofibers embossed in capillaries with periods of 416 and 278 nm from a 1 wt % solution are shown in Figure 3. For the 416 nm lines, the degree of order appeared to be comparable to that of PA **1** with nanofibers aligned in neatly spaced bundles. However, the deposition was not as uniform, with some lines completely lacking nanofibers. This characteristic was more pronounced for the finer lines (Figure 3b). In some areas, good alignment was observed for cleanly spaced bundles of small numbers of nanofibers, but in other areas the nanofibers were poorly aligned or completely absent. It is possible that in this case, the channels were too shallow and actually hindered the mobility of the nanofibers.

For the 2400 lines/mm grating, the heights of the lines produced using 5 and 1 wt % solutions were 50 ± 9and 23 ± 6 nm, respectively. The finer grating yielded line heights of 32 ± 2 and 17 ± 9 nm, respectively. Differences in line height between PAs **1** and **2** were not significant. While the difference in line height due to concentration was not surprising, the overall magnitude of the heights was larger than expected, suggesting that the nanofibers collected within the channels at concentrations of roughly 20% to 50% by volume. If the stamp was in contact with the substrate during the entire process, achieving these concentrations would require extensive mass transport down the length of the channels. This seems unlikely given that PAs **1** and **2** begin to form self-supporting gels at concentrations of 1−2% by weight.

Previous studies that applied capillary micromolding techniques most often involved positioning the stamp onto the substrate first and then placing a drop of solution at one

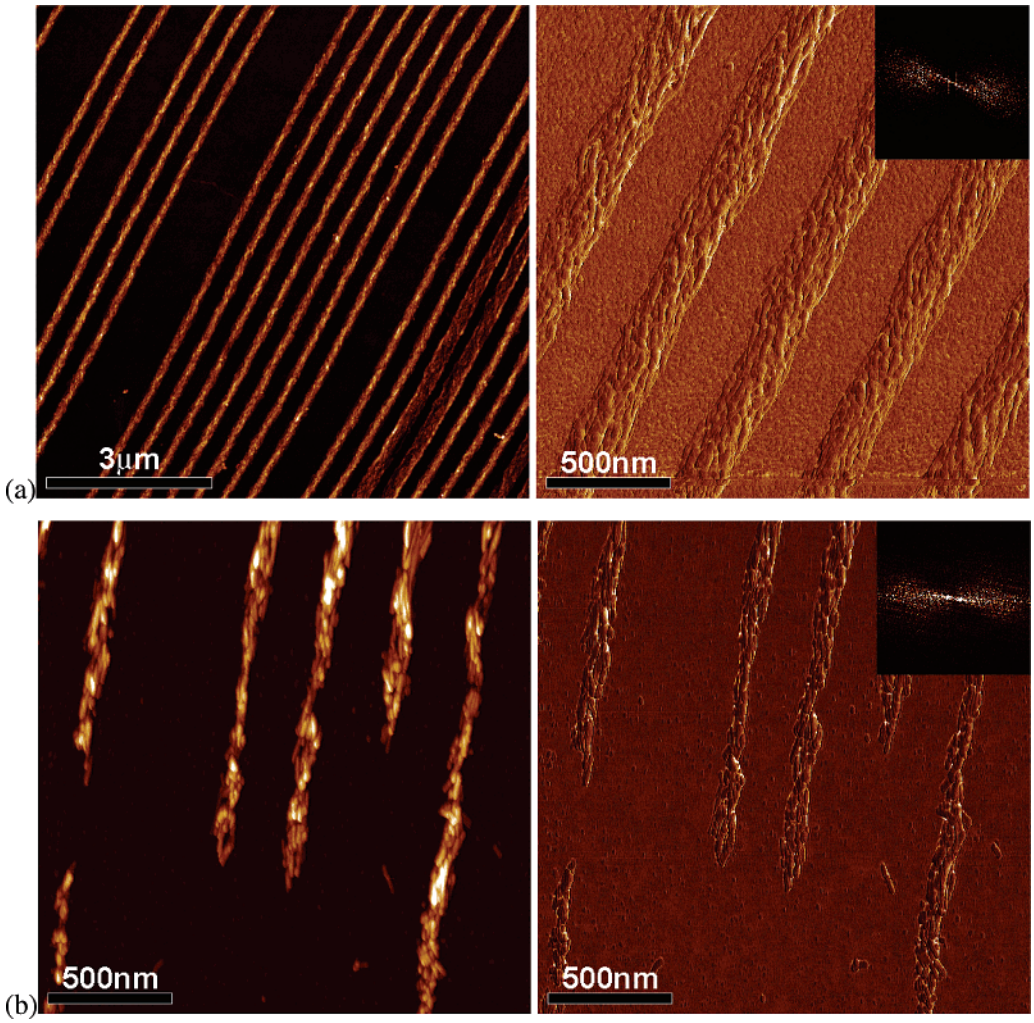

Figure 3. AFM height and phase images of aligned supramolecular nanofibers of PA **2**. The fibers were embossed from a 1 wt % solution into lines with periods of (a) 417 nm and (b) 278 nm (height scales 44.7 and 25.4 nm, respectively). In (a), the widths of the nanofiber bundles were ca. 150 nm, and the average height of the lines was 23.1 ± 0.7 nm. The inset FFT of the phase image clearly shows the periodicity of the nanofibers within each bundle oriented nearly parallel with that of the overall line pattern. In (b), the widths were ca. 50−100 nm, and the average height of the lines was 13.4 ± 1.2 nm. Overall, the degree of alignment and uniformity of deposition was poorer for the 278 nm lines than for the 416 nm lines.

of the open ends of the channels and allowing the solution to wick in by capillary action.[12,13,52−54] This method was initially attempted with PA **1**, but while the solution traveled the full length of the channels, nanofibers were only deposited about 1 mm into the channel, regardless of the initial conditions. This likely occurred because as the size and number of nanofiber aggregates increased with solvent evaporation, their diffusivity decreased. Given this observation, it is improbable that the lines deposited with the current method could result from diffusion down the confining channels. More likely, the stamp does not actually sit in contact with the substrate initially but instead on a thin film of solution several hundreds of nanometers thick. As the water evaporates, this fluid layer decreases in thickness until the stamp finally contacts the substrate, trapping a high concentration of PA nanofibers within each channel.

This mechanism also helps to explain the presence of the residual layer in Figure 2b. By AFM and SEM, the depths of the channels were 128 ± 4 and 63 ± 3 nm for the 2400 and 3600 lines/mm gratings, respectively. The smaller volume in the 278 nm channels meant that less material could be collected in them, and any nanofibers that could not be moved out from under the stamp remained as a residual layer. Furthermore, while the stiffer h-PDMS layer on the patterned surface of the stamp should reduce compression of the channel, some deformation is still expected. As such, the stamp−substrate contact area between each bundle of nanofibers was larger for the 3600 lines/mm grating, which may have decreased the actual pressure underneath the contact area.

Including an ultrasonication step in the procedure improved the overall alignment and uniformity of deposition, especially for nanofibers of PA **2**. Nonsonicated samples tended to have a thicker residual film between the channels and a greater occurrence of defects in line deposition. We suspect that mechanical agitation during the initial stages of drying imparted kinetic energy to the system, enabling the nanofibers to adopt a more equilibrium packing geometry. Ultrasonication could act on large length scales by smoothing out concentration gradients and on smaller length scales by increasing the mobility of both the supramolecular aggregates

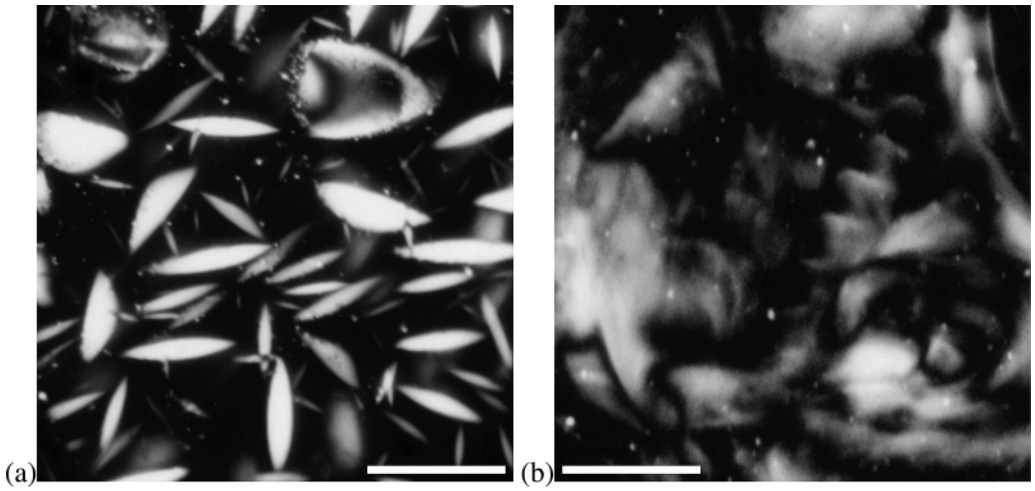

Figure 4. Polarized optical microscopy images of concentrated aqueous gels of PA nanofibers. Both scale bars are 100 μm. (a) PA **1** at roughly 15 wt % shows bright birefringence suggestive of a hexagonal liquid crystalline phase and possible phase separation from an isotropic phase. At higher concentrations, fingerprint textures indicative of a cholesteric phase can be seen, similar to those reported previously.[24] (b) PA **2** at roughly 7 wt % is more weakly birefringent but does display a texture that suggests the formation of a nematic phase.

and the molecules themselves, accelerating the process of dynamic assembly and disassembly of the nanofibers.

Nanofibers of both PAs have persistence lengths greater than 600 nm as estimated by transmission electron microscopy, SEM, and AFM images.[33,34,51] This length is longer than the dimensions of the confining capillaries, which are 416 nm wide and 128 nm tall at the largest. Because of this fact, steric hindrance likely plays a role in the alignment of the nanofibers within the channels. It is also possible that the system undergoes a phase transition to a lyotropic liquid crystalline phase as the concentration increases. Lyotropic liquid crystal models such as those put forth by Onsager[60] are particularly applicable for high aspect ratio mesogens with limited interactive forces other than steric repulsion. Figure 4 shows optical microscopy images of aqueous gels of both PAs **1** and **2** at concentrations of roughly 15% and 7% PA by weight between crossed polarizers. Both gels displayed birefringent textures that suggest self-organization of the nanofibers into nematic phases at higher concentrations. Drop cast films of both molecules showed only very limited long-range orientational order, indicating that the liquid crystalline phases are slow to organize. A liquid crystal phase is not necessary to achieve good alignment with adequate spatial confinement; however, in our systems the cooperative effect of both phenomena would improve the degree of order.

If the system indeed entered a lyotropic phase, it might be possible to observe a difference in behavior depending on solution concentration. At an Onsager transition, the material would be expected to phase separate into a dilute isotropic phase and a more concentrated nematic phase.[60] This behavior can be seen in concentrated gels of PA **1** (Figure 4a) where strongly birefringent needle-like domains on the order of tens of micrometers precipitate from a disordered medium. The "empty" lines such as those in Figure 3a and observed in samples of patterned nanofibers of both PA **1** and **2** may be due to phase separation during patterning, resulting in lines of nematic and isotropic phases. Alignment in the former would be dominated more by liquid crystalline behavior while alignment in the latter might be affected more by drying effects. When the initial solution concentration is increased from 1 to 5 wt % as shown for PA **1** in Figure 2, very few "empty" lines were seen, presumably because all of the material in solution collapsed into the condensed phase within the channels. AFM and SEM of used stamps revealed that liftoff of entire lines of nanofibers with the stamp was extremely rare, and even so, liftoff would not explain the concentration dependence.

The effectiveness of this method depends on not only the degree of order of any liquid crystalline intermediate but the dynamics of self-assembly as well. Instead of being a detriment, self-assembly during the patterning process may in fact improve the degree of order. Alignment of a covalently cross-linked fiber requires the full rotation of the whole fiber, whereas self-assembled nanofibers can break and re-form, effecting alignment with a minimum of mass transport. Differences in the degree of orientation between PA **1** and PA **2** may reflect differences in self-assembly kinetics. Despite these differences, alignment is observed in both PAs, demonstrating the promise of this method for the alignment of other self-assembling one-dimensional nanostructures.

Having found that it is possible to align PA nanofibers within parallel channels, we were interested in determining whether we could arrange the nanofibers in more complex patterns. Microchem A3 950K poly(methyl methacrylate) (PMMA) resist was spin-coated onto a silicon wafer with a 100 nm oxide layer (University Wafer). Electron-beam lithography was performed with a FEI Quanta ESEM to draw patterns in the PMMA resist film, and the topological pattern was transferred into the oxide layer by dry etching in a PlasmaLab 80 reactive ion etcher. While electron-beam lithography was time-consuming, it was required only once to create the rigid master from which the pattern could be

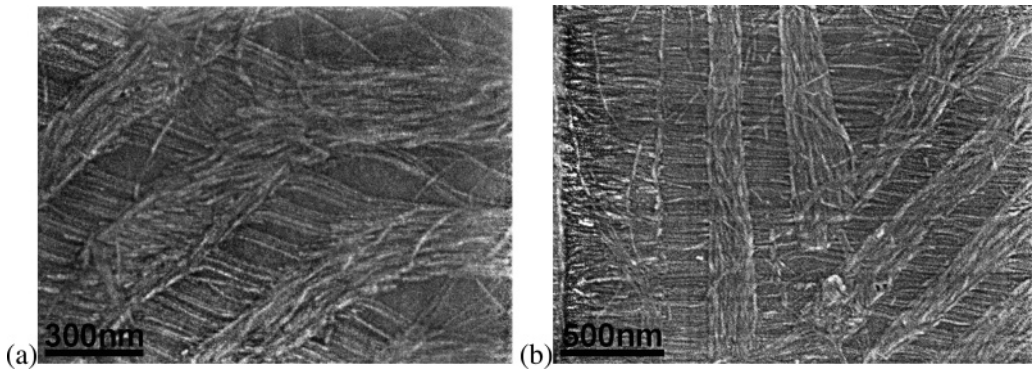

Figure 5. SEM images of nanofibers of PA **1** aligned in capillaries defined by electron-beam lithography. (a) At a 135° corner, the nanofibers were able to turn the corner without breaking. (b) At a 45° corner, most nanofibers broke before continuing in the new direction but otherwise remained aligned within the channels.

replicated multiple times by soft lithography. The pattern consisted of parallel lines 200 nm wide and spaced 200 nm apart similar to a diffraction grating, except the lines turned sharp corners periodically at angles varying from 45° to 135°. The silicon master was silanized by immersion in a 40 mM solution of octadecyltrichlorosilane (Aldrich) in toluene to prevent adhesion to PDMS and then applied in a similar manner as the commercially available diffraction gratings to mold PDMS stamps for use in solution embossing.

Figure 5 shows SEM images of nanofibers of PA **1** embossed in the electron beam defined capillaries. The nanofibers aligned along these channels just as they did in the diffraction grating molded channels. When the nanofibers reached a corner, they would either bend or break and then continue traveling parallel to the new channel direction. At a 135° turn in the channel, the nanofibers appeared to bend but remain intact as they round the corner. At sharper angles of 90° or 45°, the nanofibers usually terminated before taking up the new channel direction. The minimum radius of curvature of the nanofibers was generally observed to be about 400 nm. This is perhaps the most definitive proof that alignment in these submicrometer capillaries is due to spatial confinement and not due to any shear force generated between the stamp and the substrate. Such shear forces would likely have resulted in uniaxial alignment of the nanofibers over the substrate regardless of channel orientation.

We have previously shown that the PA self-assembles in cell media into nanofiber networks[40] and do not expect significant dissolution of the aligned nanofibers under similar conditions. Preliminary experiments do indicate that the patterns are stable in cell culture medium. Thus, they are potentially useful for studying cell behavior on bioactive substrates patterned across multiple length scales.

We have shown that PA nanofibers can be simultaneously oriented and patterned during their self-assembly from solution within microchannels. We believe this process is the result of a synergistic interaction between a liquid crystal transition and spatial confinement. The method is not limited to uniaxial alignment but can be used to guide self-assembling nanofibers around corners and in complex patterns. It is also versatile enough to be used in the alignment of other self-assembling supramolecular systems systems starting from solutions of small molecules.

Acknowledgment. This work was supported by the U.S. Department of Energy Grant DEFG02-00ER45810 and by the Nanoscale Science and Engineering Initiative of the National Science Foundation under NSF Award Number EEC-0118025. Any opinions, findings and conclusions or recommendations expressed in this material are those of the authors and do not necessarily reflect those of the National Science Foundation. This work was also supported by the National Science Foundation Graduate Research Fellowship Program and the National Defense Science and Engineering Graduate Fellowship Program. We thank the Nanoscale Integrated Fabrication, Testing and Instrumentation Center (NIFTI) for use of the AFM and the Electron Probe Instrumentation Center (EPIC) for use of the SEM at Northwestern University. The authors are grateful to Dr. James F. Hulvat for useful comments on the manuscript and to Dr. Krista L. Niece for materials synthesis and additional comments.

Supporting Information Available: Experimental methods for PDMS stamp fabrication and substrate cleaning, AFM and SEM images of the PDMS stamps after use, and SEM images of the pattern created by electron-beam lithography. This material is available free of charge via the Internet at http://pubs.acs.org.

References

(1) Alivisatos, A. P.; Barbara, P. F.; Castleman, A. W.; Chang, J.; Dixon, D. A.; Klein, M. L.; McLendon, G. L.; Miller, J. S.; Ratner, M. A.; Rossky, P. J.; Stupp, S. I.; Thompson, M. E. *Adv. Mater.* **1998**, *10*, 1297.
(2) Whitesides, G. M.; Grzybowski, B. *Science* **2002**, *295*, 2418.
(3) Hoeben, F. J. M.; Jonkheijm, P.; Meijer, E. W.; Schenning, A. *Chem. Rev.* **2005**, *105*, 1491.
(4) Muthukumar, M.; Ober, C. K.; Thomas, E. L. *Science* **1997**, *277*, 1225.
(5) Bao, Z. N.; Rogers, J. A.; Katz, H. E. *J. Mater. Chem.* **1999**, *9*, 1895.
(6) Aizenberg, J.; Black, A. J.; Whitesides, G. M. *Nature* **1999**, *398*, 495.
(7) Xia, Y. N.; Rogers, J. A.; Paul, K. E.; Whitesides, G. M. *Chem. Rev.* **1999**, *99*, 1823.
(8) Fasolka, M. J.; Mayes, A. M. *Annu. Rev. Mater. Res.* **2001**, *31*, 323.
(9) Park, C.; Yoon, J.; Thomas, E. L. *Polymer* **2003**, *44*, 6725.
(10) Segalman, R. A.; Yokoyama, H.; Kramer, E. J. *Adv. Mater.* **2001**, *13*, 1152.
(11) Xia, Y. N.; Whitesides, G. M. *Angew. Chem., Int. Ed.* **1998**, *37*, 551.
(12) Kim, E.; Xia, Y. N.; Whitesides, G. M. *Nature* **1995**, *376*, 581.
(13) Rogers, J. A.; Meier, M.; Dodabalapur, A. *Appl. Phys. Lett.* **1998**, *73*, 1766.

(14) Trau, M.; Yao, N.; Kim, E.; Xia, Y.; Whitesides, G. M.; Aksay, I. A. *Nature* **1997**, *390*, 674.
(15) Arsenault, A. C.; Rider, D. A.; Tetreault, N.; Chen, J. I. L.; Coombs, N.; Ozin, G. A.; Manners, I. *J. Am. Chem. Soc.* **2005**, *127*, 9954.
(16) Cheng, J. Y.; Mayes, A. M.; Ross, C. A. *Nat. Mater.* **2004**, *3*, 823.
(17) Dziomkina, N. V.; Vancso, G. J. *Soft Matter* **2005**, *1*, 265.
(18) vanBlaaderen, A.; Ruel, R.; Wiltzius, P. *Nature* **1997**, *385*, 321.
(19) Stutzmann, N.; Tervoort, T. A.; Broer, D. J.; Sirringhaus, H.; Friend, R. H.; Smith, P. *Adv. Funct. Mater.* **2002**, *12*, 105.
(20) Kato, T.; Mizoshita, N.; Kishimoto, K. *Angew. Chem., Int. Ed.* **2006**, *45*, 38.
(21) Binder, H.; Schmiedel, H.; Lantzsch, G.; Cramer, C.; Klose, G. *Liq. Cryst.* **1996**, *21*, 415.
(22) Crawford, G. P.; Yang, D. K.; Zumer, S.; Finotello, D.; Doane, J. W. *Phys. Rev. Lett.* **1991**, *66*, 723.
(23) Messmore, B. W.; Hulvat, J. F.; Sone, E. D.; Stupp, S. I. *J. Am. Chem. Soc.* **2004**, *126*, 14452.
(24) Sardone, L.; Palermo, V.; Devaux, E.; Credgington, D.; De Loos, M.; Marletta, G.; Cacialli, F.; Van Esch, J.; Samori, P. *Adv. Mater.* **2006**, *18*, 1276.
(25) Kim, J. S.; McHugh, S. K.; Swager, T. M. *Macromolecules* **1999**, *32*, 1500.
(26) Zhao, Y.; Fang, J. Y. *Langmuir* **2006**, *22*, 1891.
(27) Kato, T.; Kutsuna, T.; Hanabusa, K.; Ukon, M. *Adv. Mater.* **1998**, *10*, 606.
(28) Kitamura, T.; Nakaso, S.; Mizoshita, N.; Tochigi, Y.; Shimomura, T.; Moriyama, M.; Ito, K.; Kato, T. *J. Am. Chem. Soc.* **2005**, *127*, 14769.
(29) Kato, T.; Kutsuna, T.; Yabuuchi, K.; Mizoshita, N. *Langmuir* **2002**, *18*, 7086.
(30) Lee, K. C.; Carlson, P. A.; Goldstein, A. S.; Yager, P.; Gelb, M. H. *Langmuir* **1999**, *15*, 5500.
(31) Yu, Y. C.; Berndt, P.; Tirrell, M.; Fields, G. B. *J. Am. Chem. Soc.* **1996**, *118*, 12515.
(32) Yamada, N.; Koyama, E.; Imai, T.; Matsubara, K.; Ishida, S. *Chem. Commun.* **1996**, 2297.
(33) Hartgerink, J. D.; Beniash, E.; Stupp, S. I. *Science* **2001**, *294*, 1684.
(34) Niece, K. L.; Hartgerink, J. D.; Donners, J.; Stupp, S. I. *J. Am. Chem. Soc.* **2003**, *125*, 7146.
(35) Behanna, H. A.; Donners, J.; Gordon, A. C.; Stupp, S. I. *J. Am. Chem. Soc.* **2005**, *127*, 1193.
(36) Hartgerink, J. D.; Beniash, E.; Stupp, S. I. *Proc. Natl. Acad. Sci. U.S.A.* **2002**, *99*, 5133.
(37) Jiang, H. Z.; Guler, M. O.; Stupp, S. I. *Soft Matter* **2007**, *3*, 454.
(38) Paramonov, S. E.; Jun, H. W.; Hartgerink, J. D. *J. Am. Chem. Soc.* **2006**, *128*, 7291.
(39) Tovar, J. D.; Claussen, R. C.; Stupp, S. I. *J. Am. Chem. Soc.* **2005**, *127*, 7337.
(40) Silva, G. A.; Czeisler, C.; Niece, K. L.; Beniash, E.; Harrington, D. A.; Kessler, J. A.; Stupp, S. I. *Science* **2004**, *303*, 1352.
(41) Rajangam, K.; Behanna, H. A.; Hui, M. J.; Han, X. Q.; Hulvat, J. F.; Lomasney, J. W.; Stupp, S. I. *Nano Lett.* **2006**, *6*, 2086.
(42) Agheli, H.; Malmstrom, J.; Larsson, E. M.; Textor, M.; Sutherland, D. S. *Nano Lett.* **2006**, *6*, 1165.
(43) Falconnet, D.; Csucs, G.; Grandin, H. M.; Textor, M. *Biomaterials* **2006**, *27*, 3044.
(44) Kane, R. S.; Takayama, S.; Ostuni, E.; Ingber, D. E.; Whitesides, G. M. *Biomaterials* **1999**, *20*, 2363.
(45) Lee, K. B.; Park, S. J.; Mirkin, C. A.; Smith, J. C.; Mrksich, M. *Science* **2002**, *295*, 1702.
(46) Stevens, M. M.; George, J. H. *Science* **2005**, *310*, 1135.
(47) Sullivan, T. P.; van Poll, M. L.; Dankers, P. Y. W.; Huck, W. T. S. *Angew. Chem., Int. Ed.* **2004**, *43*, 4190.
(48) Whitesides, G. M.; Ostuni, E.; Takayama, S.; Jiang, X. Y.; Ingber, D. E. *Annu. Rev. Biomed. Eng.* **2001**, *3*, 335.
(49) Denis, F. A.; Pallandre, A.; Nysten, B.; Jonas, A. M.; Dupont-Gillain, C. C. *Small* **2005**, *1*, 984.
(50) Wilson, D. L.; Martin, R.; Hong, S.; Cronin-Golomb, M.; Mirkin, C. A.; Kaplan, D. L. *Proc. Natl. Acad. Sci. U.S.A.* **2001**, *98*, 13660.
(51) Jiang, H. Z.; Stupp, S. I. *Langmuir* **2005**, *21*, 5242.
(52) Zhang, F. L.; Nyberg, T.; Inganas, O. *Nano Lett.* **2002**, *2*, 1373.
(53) Roman, L. S.; Inganas, O.; Granlund, T.; Nyberg, T.; Svensson, M.; Andersson, M. R.; Hummelen, J. C. *Adv. Mater.* **2000**, *12*, 189.
(54) Donthu, S. K.; Pan, Z.; Shekhawat, G. S.; Dravid, V. P.; Balakrisnan, B.; Tripathy, S. *J. Appl. Phys.* **2005**, *98*, 024304.
(55) Pierschbacher, M. D.; Ruoslahti, E. *Proc. Natl. Acad. Sci. U.S.A.: Biol. Sci.* **1984**, *81*, 5985.
(56) Pierschbacher, M. D.; Ruoslahti, E. *Nature* **1984**, *309*, 30.
(57) Sephel, G. C.; Tashiro, K. I.; Sasaki, M.; Greatorex, D.; Martin, G. R.; Yamada, Y.; Kleinman, H. K. *Biochem. Biophys. Res. Commun.* **1989**, *162*, 821.
(58) Tashiro, K.; Sephel, G. C.; Weeks, B.; Sasaki, M.; Martin, G. R.; Kleinman, H. K.; Yamada, Y. *J. Biol. Chem.* **1989**, *264*, 16174.
(59) Odom, T. W.; Love, J. C.; Wolfe, D. B.; Paul, K. E.; Whitesides, G. M. *Langmuir* **2002**, *18*, 5314.
(60) De Gennes, P. G.; Prost, J. *The Physics of Liquid Crystals*, 2nd ed.; Oxford University Press: Oxford, 1993.

NL062835Z